

the complexity of the network make it impossible. Practically, the accuracy and complexity of the load model are determined based on the type of system studies and available technical capabilities. For example, in load flow studies, a simple model of constant power is used as the load model. In dynamic studies, it is appropriate to use a model that represent load variations over time in terms of network fundamental variables; i.e., voltage and frequency [6, 7].

Due to the high diversity and complexity of power system loads, it is challenging to provide a complete load model. Various methods have been proposed, which can be broadly categorized into two main methods [8]: static modelling and dynamic modelling. In static modelling, only the steady state relationship between active and reactive power with voltage and frequency is considered. While dynamic modelling considers the transient behaviour of the load after changes in voltage or frequency [9]. However, the static load model can also be applied for modelling dynamic loads using a time-varying static model [10, 11].

Generally, two main approaches have been addressed in static load modelling studies for a medium voltage distribution feeder [12, 13]: measurement-based approach and component-based approach. In measurement-based approaches, measurement devices are required to determine the sensitivity of active and reactive power of electrical loads to voltage and frequency variations. The advantage of this approach is that it provides real-time information about the loads. However, the high cost of installing, maintaining, and repairing measurement devices poses main challenges in using this method. In component-based approaches, different loads connected to a feeder are individually considered and a specific load model is determined for all loads with similar active and reactive power sensitivity to voltage and frequency variations. Consequently, the loads on a feeder are modelled as a composite load [14]. The major drawback of this approach is the need for extensive information to determine the types and models of loads connected to the feeder.

In [15], the polynomial model is used to load modelling. Authors in [16], proposed load modelling using the exponential dynamic load model at the selected bus. However, the polynomial model cannot be accurate, particularly for exponents bigger than two, such as motor loads. The least square error method is used in [17] to dynamic load modelling for bulk load. However, the proposed method in [17] needs synchrophasors with wide area measurement system. Authors in [18] proposed a combination of static and dynamic model that model parameters are determined using PSO algorithm for modelling of industrial substation loads.

In this paper, a case study is presented for accurate static modelling of a medium voltage distribution feeder considering practical constraints. The proposed method based on curve fitting and practical measurement data to select the appropriate time interval for determining accurate load model coefficients is the main contribution of this study. The obtained results show that using the proposed method, the normalized root mean square error (NRMSE) between the actual recorded and estimated power consumption during tap changes is less than 0.5%.

2. ZIP polynomial model

The static characteristics of loads can be classified into three categories: constant power, constant current, and constant impedance. Additionally, the classification takes into consideration the active and reactive power dependency on voltage. For a load with constant impedance, the power dependency on voltage is modelled as a quadratic function. For a load with constant current, the power dependency is linear. And for a load with constant power, there is no voltage dependency. The ZIP model, represented by equations (1) and (2), is a polynomial model that combines these categorizations [19].

$$P = P_0 \left(Z_p \left(\frac{V}{V_0} \right)^2 + I_p \left(\frac{V}{V_0} \right) + P_p \right) \quad (1)$$

$$Q = Q_0 \left(Z_q \left(\frac{V}{V_0} \right)^2 + I_q \left(\frac{V}{V_0} \right) + P_q \right) \quad (2)$$

In the ZIP model, P_0 , Q_0 , and V_0 represent the initial values from the studied system (nominal conditions), and Z_p , I_p , P_p , Z_q , I_q , and P_q are the coefficients of the ZIP model.

To determine the accurate coefficients of a ZIP model using curve fitting, it is necessary to determine the acceptable range of the coefficients and the stable region of the PV and QV curves. By considering equation (1) and introducing $V = (V/V_0)$ as a normalized voltage factor, and eliminating the factor P_0 , equation (1) can be simplified to equation (3).

$$P = Z_p V^2 + I_p V + P_p \quad (3)$$

By applying the second derivative of equation (3), and considering the stable region of the PV curve shown in Fig. 1, the acceptable range of the Z_p coefficient can be determined as follows.

$$\frac{d^2 P}{d^2 V} = 2Z_p \Rightarrow 2Z_p > 0 \Rightarrow Z_p > 0 \quad (4)$$

Since constant current loads are linearly related to the voltage, by applying the first derivative of equation (3), and considering the positive value of Z_p and V , the acceptable range of the I_p coefficient can be obtained:

$$\frac{dP}{dV} = 2Z_p V + I_p > 0 \Rightarrow I_p < 0 \quad (5)$$

Considering equation (5) equal to zero, the minimum stable voltage can be deduced:

$$V_{min} = \frac{-I_p}{2Z_p} \quad (6)$$

Based on the positivity of the minimum active power passing through the radial distribution feeders and the minimum stable voltage, it can be stated:

$$P_{min} = Z_p V_{min}^2 + I_p V_{min} + P_p > 0 \quad (7)$$

$$P_{min} = Z_p \left(\frac{-I_p}{2Z_p} \right)^2 + I_p \left(\frac{-I_p}{2Z_p} \right) + P_p > 0 \quad (8)$$

$$P_{min} = \frac{I_p^2}{4Z_p} - \frac{I_p^2}{2Z_p} + P_p > 0 \quad (9)$$

$$P_{min} = \frac{-I_p^2}{4Z_p} + P_p > 0 \Rightarrow P_p > \frac{I_p^2}{4Z_p} \quad (10)$$

It is important to note that the following equality constraint must be observed between ZIP coefficients:

$$Z_p + I_p + P_p = 1 \quad (11)$$

Considering that the stable range of reactive power, as depicted in Fig. 2, can also include negative values, the coefficients Z_q , I_q , and P_q can be positive or negative. Therefore, there is no need to determine a specific range for these coefficients.

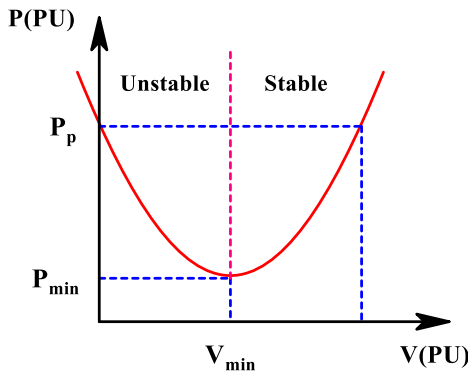


Fig. 1. Typical PV curve.

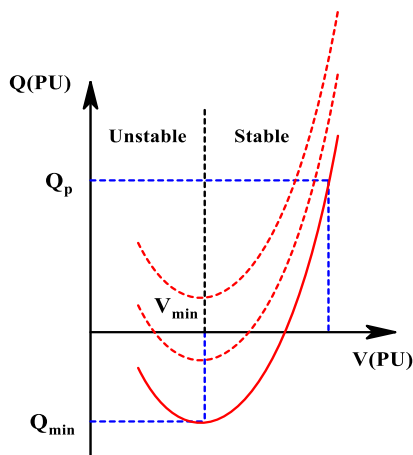


Fig. 2. Typical QV curve.

3. Problem solving method

To solve the problem and obtain the coefficients of the ZIP model, the least squares method described in (12) is used:

$$\min_x \sum_{i=1}^n (F(x, xdata_i) - ydata_i)^2 \quad (12)$$

In this equation, $ydata$ represents the measured active and reactive power data and $xdata$ represents the measured voltage values. These data are weighted by the variances, which are provided as priors.

For the purpose of accurate static load modelling and analysis of the modelling results, the data of a medium voltage distribution feeder (Khourin-Kermanshah) with one-second time interval measurement has been considered as a case study. Additionally, to enhance the modelling accuracy, the tap position of the upstream

substation transformer of this feeder has been altered during the measurement period. Fig. 3 to Fig. 5 depict the values of active power, reactive power, and voltage of the Khourin feeder in the studied period, respectively.

To determine the time intervals for determining the coefficients of the ZIP load model, the voltage, active power, and reactive power values are first presented in per unit. Fig. 6 and Fig. 7 illustrate the voltage, active power, and reactive power of the Khourin feeder load in per unit.

Considering the time interval of tap changes (from 10:49:37 to 10:50:37 as seen in Fig. 5) and the variations of active power and reactive power in relation to voltage changes, the following time intervals are considered for calculating the load model coefficients and analysing the results:

1. First-time interval: The entire time interval of 242 seconds, considering a sampling rate of one minute (in this case, there are 5 data points used for modelling).
2. Second-time interval: A 60-second time interval before the tap changes, considering a sampling rate of one second.
3. Third-time interval: A 60-second time interval during the tap changes, considering a sampling rate of one second.



Fig. 3. Active power of Khourin feeder in the studied period.

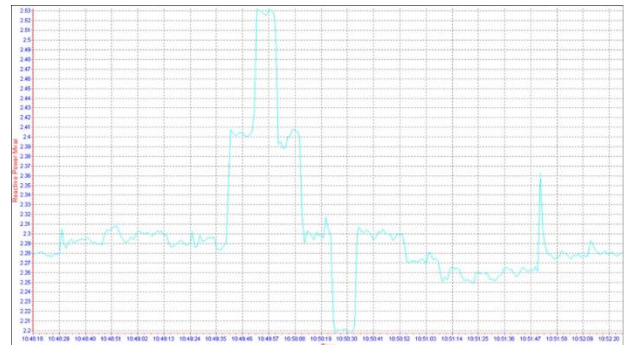


Fig. 4. Reactive power of Khourin feeder in the studied period.

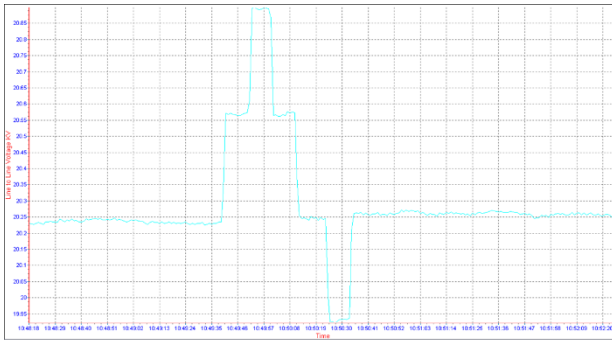


Fig. 5. Khourin feeder voltage in the studied period.

4. Third-time interval: A 60-second time interval during the tap changes, considering a sampling rate of one second.
5. Fourth-time interval: A 60-second time interval after the tap changes, considering a sampling rate of one second.
6. Fifth-time interval: The entire time interval of 242 seconds, considering a sampling rate of one second.

The coefficients of the ZIP load model and the value of the normalized root mean square error (NRMSE) for each mentioned time intervals are presented in Tables I and II. The NRMSE value is calculated using the following equation:

$$NRMSE = \frac{\sqrt{\frac{\sum_{i=1}^n (\hat{y}_i - y_i)^2}{n}}}{\bar{y}} \times 100 \tag{13}$$

In this equation, \hat{y}_i represents the calculated values from the model, y_i represents the measured values, and \bar{y} represents the mean of the measured values (for active and reactive power).

As observed in Tables I and II, the minimum value of NRMSE is related to the third-time interval (during the tap changes). In this time interval, the NRMSE value for the active power model is approximately 0.22%, and for the reactive power model, it is around 0.34%. Additionally, the maximum modelling error is associated with the first-time interval. In this time interval, the NRMSE value for the active power model is approximately 1.45%, and for the reactive power model, it is around 1.04%. After the first-time interval, the fifth- and fourth-time intervals have the highest modelling errors, respectively. If we extend the obtained model from the first to the fourth-time intervals to the entire time interval of 242 seconds, the modelling errors for each time interval, according to Tables I and II, would increase. Specifically, the NRMSE values for the active power model in the first to fourth-time intervals would increase to approximately 1.46%, 1.82%, 1.52%, and 1.92%, respectively. Similarly, the NRMSE values for the reactive power model in the first to fourth-time intervals would increase to approximately 1.97%, 0.97%, 0.86%, and 2.93%, respectively.

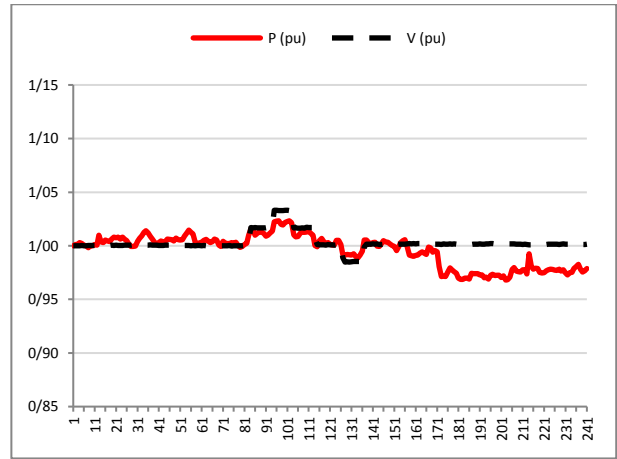


Fig. 6. Voltage and active power of the Khourin feeder in per unit.

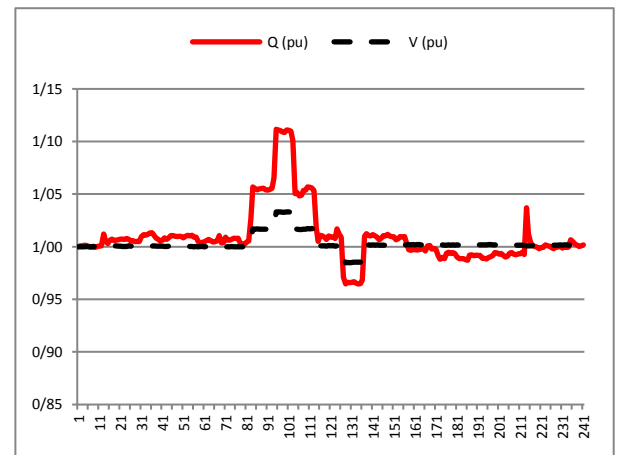


Fig. 7. Voltage and reactive power of the Khourin feeder in per unit.

Table I. Coefficients of the ZIP load model for active power and NRMSE values for different time intervals.

Time interval	Zp	Ip	Pp	NRMSE (%)	NRMSE (%) (1-242 sec)	NRMSE (%) (1-171 sec)
1	1.179	-1.365	1.179	1.449	1.463	-
2	1.024	-0.994	0.974	0.390	1.826	0.770
3	0.790	-0.966	1.177	0.221	1.526	0.455
4	0.791	-0.603	0.791	1.254	1.928	-
5	0.881	-1.007	1.119	1.336	1.336	-

Table II. Coefficients of the ZIP load model for reactive power and NRMSE values for different time intervals.

Time interval	Zq	Iq	Pq	NRMSE (%)	NRMSE (%) (1-242 sec)	NRMSE (%) (1-171 sec)
1	1.1820	-1.363	1.181	1.043	1.974	-
2	2.128	-1.123	1.7E-10	0.356	0.966	0.517
3	2.095	-1.257	0.165	0.347	0.857	0.518
4	1.082	-1.181	1.082	0.675	2.927	-
5	1.698	-0.696	2.6E-05	0.881	0.881	-

If we exclude the time interval after the tap changes and extend the obtained model from the second and third-time intervals to the first 171 seconds, it can be observed that the NRMSE values for the active power model in the second and third-time intervals would be approximately 0.77% and 0.46%, respectively. Furthermore, the NRMSE value for the reactive power model in the second and third-time intervals would be around 0.52%.

4. Analysing the results of Khourin feeder load modelling

As observed, the coefficients of the load model and the magnitude of modelling errors are significantly influenced by the selected time interval and the number of data used. In order to analyse the reasons for these differences, the curves of the obtained models, along with the measured data, are plotted in Fig. 8 to Fig. 11.

Fig. 8 illustrates the PV curve for different load models along with the measured active powers for various voltage values. As observed, the different curves are closely aligned within the recorded voltage range (from 0.985 to 1.033 per unit). For better clarity, the mentioned curves are displayed in Fig. 9 within the voltage range of 0.97 to 1.05 per unit. As observed in Fig. 9, during the tap changes (the third-interval), the active power varies proportionally with the voltage change, and the measurement data (black star markers) are scattered across the entire voltage variation range. Therefore, the modelling error percentage is minimal (0.22%), and the corresponding fitted curve (black curve) appropriately fits the measurement data.

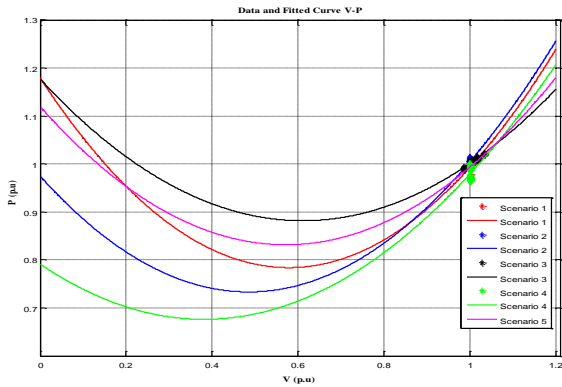


Fig. 8. PV curve for different load models.

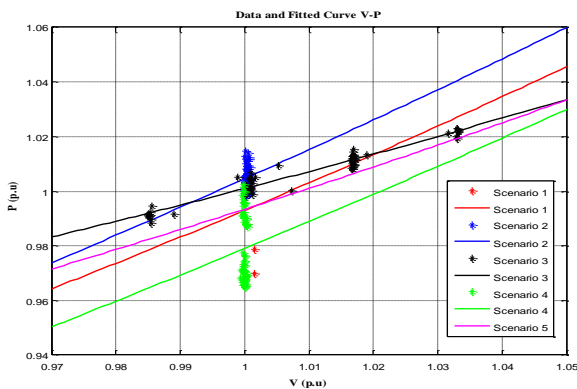


Fig. 9. Zoomed PV curve for different load models.

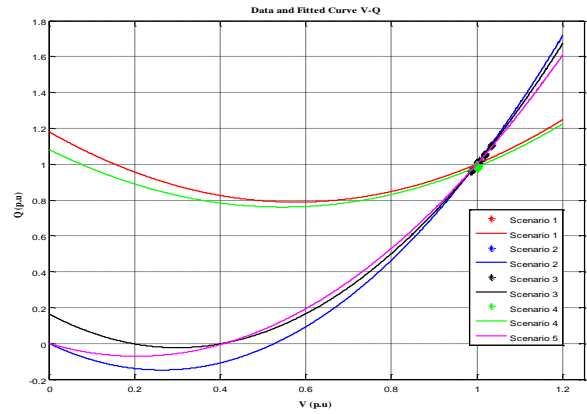


Fig. 10. QV curve for different load models.

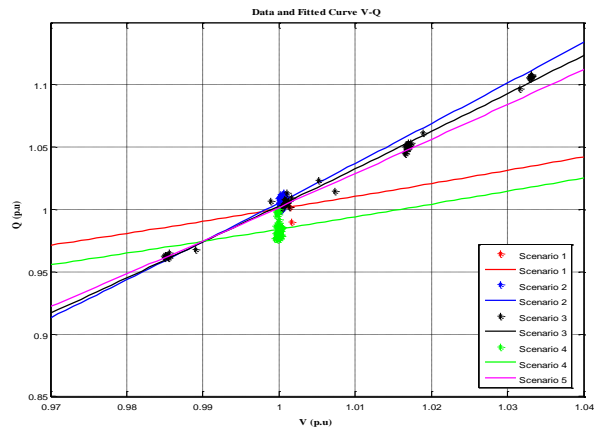


Fig. 11. Zoomed QV curve for different load models.

In the second-interval (before the tap changes) and the fourth-interval (after the tap changes), as shown in Fig. 9, although the voltage remains relatively constant, the active power varies. However, the magnitude of the active power variation in the fourth-interval is much larger than that in the second-interval. As can be seen in Fig. 6 and Fig. 7, in these two time-intervals the voltage variations are very small and the voltage value is approximately 1 pu. For this reason, the modelling error increases in the second and fourth-intervals compared to the third-interval. Furthermore, since the range of active power variations in the fourth-interval is greater, the error magnitude in this interval is also higher than that in the second-interval.

In the first and fifth-intervals, the fourth-time interval data are also included in the calculation of the model coefficients. As a result, the error increases in these time-intervals.

In the same manner, the reasons for the different coefficients of various load models and the different NRMSE in the studied time-intervals for reactive power can be analysed. Fig. 10 and Fig. 11 respectively illustrate the QV curves and their magnified view for different load models.

5. Conclusion and discussion

In this paper, a medium voltage distribution feeder is modelled as a static ZIP load. The static load model is determined using curve fitting. To attain an accurate load model, the acceptable range of model coefficients must be determined first. The obtained results confirm that where

the load changes without a noticeable voltage variation, the modelling error increases, and it is necessary to perform re-modelling at each load level. Additionally, the best temporal fitting is achieved when the voltage range is varied using tap changes, and the effect of voltage variation on active and reactive power consumption is observed. The obtained results for an actual medium voltage distribution feeder (Khourin-Kermanshah) show that using the proposed method, the NRMSE between the actual recorded and estimated power consumption during tap changes is less than 0.5%. Although the proposed method accurately models the load of a feeder in the range of tap changes, the implementation of the proposed method faces some limitations. Since the load level varies at different times, continuous tap changes (to determine the appropriate load model) are practically not feasible. Furthermore, due to the limited range of tap variation, the obtained load model is accurate only within a limited voltage range. On the other hand, to extract the appropriate load model for different feeders in the system, a large number of measurement devices with the capability of storing data in small time intervals are required.

6. References

- [1]. R. A. Asl, A. A. Asl, "A new approach to load modelling for a power electronics - based load structure", *The Journal of Engineering*, no. 6, e12283, 2023.
- [2]. A. S. Jović, L. M. Korunović, S. Z. Djokic, "Application of meteorological variables for the estimation of static load model parameters", *Energies*, vol. 14, no. 16, 4874, 2021.
- [3]. A. Bokhari, A. Alkan, R. Dogan, M. Diaz-Aguiló, F. De Leon, D. Czarkowski, R. E. Uosef, "Experimental determination of the ZIP coefficients for modern residential, commercial, and industrial loads", *IEEE Transactions on Power Delivery*, vol. 29, no. 3, p.p. 1372-1381, 2013.
- [4]. E. Vaahedi, M. A. El-Kady, J. A. Libaque-Esaine, V. F. Carvalho, "Load models for large-scale stability studies from end-user consumption", *IEEE transactions on power systems*, vol. 2, no. 4, p.p. 864-870, 1987.
- [5]. L. M. Korunović, A. S. Jović, S. Z. Djokic, "Measurement-based evaluation of static load characteristics of demands in administrative buildings", *International Journal of Electrical Power & Energy Systems*, vol. 118, 105782, 2020.
- [6]. B. K. Choi, H. D. Chiang, Y. Li, H. Li, Y. T. Chen, D. H. Huang, M. G. Lauby, "Measurement-based dynamic load models: derivation, comparison, and validation", *IEEE Transactions on Power Systems*, vol. 21, no. 3, p.p. 1276-1283, 2006.
- [7]. A. Karimipouya, S. Karimi, H. Abdi, "Induction motor modelling for load-frequency control system", *Journal of Energy Management and Technology*, vol. 6, no. 3, 136-144, 2022.
- [8]. P. Ju, C. Qin, F. Wu, H. Xie, Y. Ning "Load modeling for wide area power system", *International Journal of Electrical Power & Energy Systems*, vol. 33, no. 4, 909-917, 2011.
- [9]. P. Kundur, "Power system stability and control", New York: McGraw-hill, 1994.
- [10]. EPRI Report, "Measurement - based load modeling", Product ID: 1014402, 2006.
- [11]. J. R. Ribeiro, F. J. Lange, "A new aggregation method for determining composite load characteristics", *IEEE Transactions on Power Apparatus and Systems*, vol. 8, p.p. 2869-2875, 1982.
- [12]. W. W. Price, K. A. Wirgau, A. Murdoch, J. V. Mitsche, E. Vaahedi, M. El-Kady, "Load modeling for power flow and transient stability computer studies", *IEEE Transactions on Power Systems*, vol. 3, no. 1, p.p. 180-187, 1988.
- [13]. J. Hou, Z. Xu, Z. Y. Dong, "Load modeling practice in a smart grid environment", *4th International Conference on Electric Utility Deregulation and Restructuring and Power Technologies (DRPT)*, pp. 7-13, 2011.
- [14]. W. W. Price, S. G. Casper, C. O. Nwankpa, R. W. Bradish, H. D. Chiang, C. Concordia, G. Wu, "Bibliography on load models for power flow and dynamic performance simulation", *IEEE Power Engineering Review*, vol. 15, no. 2, 1995.
- [15]. A. S. Carneiro, et al., "Static load modeling based on field measurements", *IEEE Manchester PowerTech*, 2017.
- [16]. E. Polykarpou, M. Asprou, E. Kyriakides, "Dynamic load modelling using real time estimated states", *IEEE Manchester PowerTech*, 2017.
- [17]. M. K. Hasan, M. M. Ahmed, N. F. Wani, A. H. Abbas, L. M. Alkwai, S. Islam, A.K.M. Ahasan Habib, R. Hassan, "Dynamic load modelling for bulk load using synchrophasors with wide area measurement system for smart grid real-time load monitoring and optimization", *Sustainable Energy Technologies and Assessments*, vol. 57, 103190, 2023.
- [18]. A. Bali, H. Abdi, A. Rostami, S. Karimi, "Load modeling based on real data applying PSO algorithm", *Majlesi Journal of Electrical Engineering*, vol. 13, no. 3, p.p. 15-25, 2019.
- [19]. H. Abdi, M. Moradi, S. Karimi, "Analyzing the load modelling impacts on uncertain optimal reactive power dispatch problem by using grey wolf optimization", *Modeling and Simulation in Electrical and Electronics Engineering*, vol. 1, no. 3, p.p. 27-34, 2021.